Journal of Innovative Optical Health Sciences
Vol. 12, No. 2 (2019) 1950003 (11 pages)

DOI: 10.1142/S1793545819500032

Identification and analysis of serum samples by surface-enhanced Raman spectroscopy combined with characteristic ratio method and PCA for gastric cancer detection

Liu Guo*, Yuanpeng Li*, Furong Huang*,§,¶,**, Jia Dong*, Fucui Li*, Xinhao Yang*, Siqi Zhu* and Maoxun Yang†,‡,‖,**

*Department of Opto-Electronic Engineering
Jinan University, Guangzhou 510632, P. R. China

†Zhuhai Da Hengqin Science and Technology Development Co., Ltd
Hengqin New Area, Zhuhai 519000, P. R. China

‡Zhuhai Hopegenes Medical & Pharmaceutical Institute Co., Ltd
Hengqin New Area, Zhuhai 519000, P. R. China

§Research Institute of Jinan University in Dongguan
Dongguan 523000, P. R. China
¶furong_huang@163.com
‖yangmaoxun1980@163.com

Received 11 July 2018
Accepted 10 December 2018
Published 10 January 2019

This study aimed to explore the application of surface-enhanced Raman scattering (SERS) in the rapid diagnosis of gastric cancer. The SERS spectra of 68 serum samples from gastric cancer patients and healthy volunteers were acquired. The characteristic ratio method (CRM) and principal component analysis (PCA) were used to differentiate gastric cancer serum from normal serum. Compared with healthy volunteers, the serum SERS intensity of gastric cancer patients was relatively high at 722 cm^{-1}, while it was relatively low at 588, 644, 861, 1008, 1235, 1397, 1445 and 1586 cm^{-1}. These results indicated that the relative content of nucleic acids in the serum of gastric cancer patients rises while the relative content of amino acids and carbohydrates decreases. In PCA, the sensitivity and specificity of discriminating gastric cancer were 94.1% and 94.1%, respectively, with the accuracy of 94.1%. Based on the intensity ratios of four characteristic peaks at 722, 861, 1008 and 1397 cm^{-1}, CRM presented the diagnostic sensitivity and specificity of 100% and 97.4%, respectively, and the accuracy of 98.5%. Therefore, the three peak intensity ratios of I_{722}/I_{861}, I_{722}/I_{1008} and I_{722}/I_{1397} can be considered as biological fingerprint

**Corresponding authors.

information for gastric cancer diagnosis and can rapidly and directly reflect the physiological and pathological changes associated with gastric cancer development. This study provides an important basis and standards for the early diagnosis of gastric cancer.

Keywords: Surface-enhanced Raman spectroscopy; serum; gastric cancer; characteristic ratio method; principal components analysis.

1. Introduction

Gastric cancer is currently the fourth most common malignancy and the second leading cause of cancer-related deaths worldwide. Approximately 650,000 individuals have died from this type of cancer, and 880,000 new cases of gastric cancer are diagnosed each year. Improving the diagnosis of gastric cancer is the most important approach to reducing the mortality rate of this malignancy.[1,2] Endoscopy combined with histopathological analysis is the most accurate method for the diagnosis of gastric cancer. This method, however, inflicts damage on patients. In addition, the subjectivity of pathological diagnosis and the uncertainty of endoscopic positioning are unavoidable and often result in the misdiagnosis of small lesions in the early stage of gastric cancer.[3–5] Therefore, identifying a highly sensitive, rapid, and noninvasive screening method for the diagnosis of gastric cancer is vital.[6–8]

Near-infrared Raman spectroscopy can be used to monitor the changes associated with the development of diseases because it reflects differential changes in biomolecules, such as proteins, carbohydrates and lipids.[9,10] Surface-enhanced Raman scattering (SERS) spectra has considerable potential as a cancer detection method given its high specificity and sensitivity.[11–13] In the field of biomedicine, in recent years, SERS technique has shown to be an excellent technique for the biopsy-based and body-fluid-based detection of some cancers such as gastric cancer, breast cancer, colorectal cancer, esophagus cancer and cervical cancers.[14–20] It has demonstrated good application value in the body-fluid-based detection of cancer and is expected to provide new diagnostic criteria for the clinical detection and study of cancer.[21] Among the body fluids detection, the applications of blood detection are the most frequent.[22] Many research teams have attempted to utilize the SERS technique in blood-based cancer detection. Feng *et al.* used a polarized laser to acquire the plasma SERS spectra of healthy volunteers and gastric cancer patients, and combined the multivariate statistical methods of principal component analysis (PCA) and linear discriminant analysis (LDA) to distinguish the blood samples of healthy volunteers from those of cancer patients. The diagnostic sensitivity and specificity were 79.5% and 91%, respectively. The results proved that the healthy volunteers and the gastric cancer patients can be differentiated by the SERS spectra of human plasma.[23] Vargas-Obieta *et al.* collected the SERS spectra of the serum samples of 14 controls and 14 breast cancer patients and demonstrated that SERS and PCA-LDA can be used to discriminate between control and cancer samples with 96% sensitivity and 87% specificity.[24] Sánchez-Rojo *et al.* collected serum SERS spectra of 14 controls and 14 cervical cancer patients. The spectral data was processed using multivariate statistical analysis including principal component analysis (PCA) and LDA, and the sensitivity and specificity for correctly classifying control and cervical cancer samples were both 88%.[25]

PCA and LDA are the main mathematical statistical methods used for cancer detection based on Raman spectroscopy.[26] Given the complexity of multidimensional analyses and the massive size of spectral data, a simple and accurate multivariate statistical method for the rapid detection of cancer in body fluid must be developed on the basis of the SERS technique.[27] The characteristic ratio method (CRM) is a popular unsupervised statistical analysis method that discriminates samples by correlating variations in sample spectra with sample pathology on the basis of peak intensity ratios. CRM is simpler and faster than PCA. Thus, a diagnostic method that combines SERS with CRM may have potential clinical applications in the diagnosis of gastric cancer.

In this study, serum samples collected from 34 healthy volunteers and 34 patients who had been diagnosed with gastric cancer through histopathological methods were used as the research objects. Gold nanoparticles were used as the enhancement

base. The differences in SERS spectra between gastric cancer patients and healthy volunteers were compared to study the changes in serum substance concentrations. Finally, the CRM and PCA were used to distinguish the SERS spectra of the serum samples of normal and gastric cancer patients for the rapid diagnosis of gastric cancer.

2. Experimental Materials and Methods

2.1. *Preparation and characterization of gold colloids*

Gold colloids were prepared by using sodium citrate to restore chloroauric acid. A total of 100 ml of 0.01% chloroauric acid solution was boiled on a heated magnetic stirring apparatus. The solution was then removed from the stirring apparatus, mixed with 1 ml of 1% sodium citrate, then stirred and heated for 15 min. A wine-red gold sol solution was obtained after intense boiling and cooling. The solution was centrifuged for further use. The gold sol was dropped to the microscope slide and dried for further measurement.

Figure 1 showed the extinction spectrum and the image of scanning electron microscope of the gold sol prepared in the trial. It was measured with ultraviolet and visible spectrophotometer (supplied by Shimadzu Corporation, with model of UV-2550), and the absorption peak of the gold sol was located at 520 nm, and its measured spectral bandwidth from 300 to 900 nm. The gold sol was further measured using the field emission scanning electron microscope (supplied by German Zeiss, with the model of ultra55), which showed that the average diameter of the gold sol was of 40 ± 3 nm.

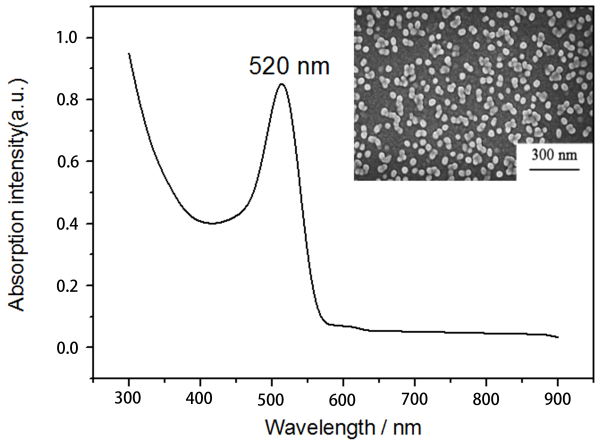

Fig. 1. The UV/Visible absorption spectrum of the Au colloid. The absorption maximum is located at 520 nm. The inserted picture is the the TEM micrograph of the Au nanoparticles.

2.2. *Preparation of human serum samples*

A total of 68 serum samples were collected from the patients of The First Affiliated Hospital of Jinan University. Among these samples, 34 were collected from patients who were newly diagnosed with gastric cancer, and 34 were collected from healthy volunteers. The mean age of patients with gastric cancer was 53 ± 10 years, whereas that of healthy volunteers was 48 ± 12 years. All samples were collected from patients with the same racial and socioeconomic backgrounds. Serum were mixed with gold colloid suspension at the volume ratio of 1:2, maintained at 4°C for 2 h, and then transferred to a cuvette for SERS detection.

2.3. *Raman instrumentation*

A portable Raman spectrometer was used as the measurement instrument. The measurement parameters were as follows: excitation wavelength of 785 nm, power of 70 mW, spectral resolution of 8 cm^{-1}, and spectral window of 400–1800 cm^{-1}.

Given that the acquired Raman spectra exhibited baseline drift and measurement was affected by random noise, the 400–1800 cm^{-1} region in Raman spectra was subjected to background subtraction and smoothing using Origin 8.5 software.

3. Results and Discussion

3.1. *Analysis of serum surface-enhanced Raman scattering (SERS) spectra*

The averaged conventional Raman spectra of serum samples from 34 healthy volunteers and 34 gastric cancer patients are shown in Fig. 2. The Raman spectra of the serum were collected at integration times of 10, 20, 30 and 60 s. It can be seen that no obvious Raman signal is detected in both normal and gastric cancer serum without using gold nanoparticles. The Raman signals are negligibly enhanced with the prolongation of integration time. A slight baseline drift is observed at the integration time of 60 s.

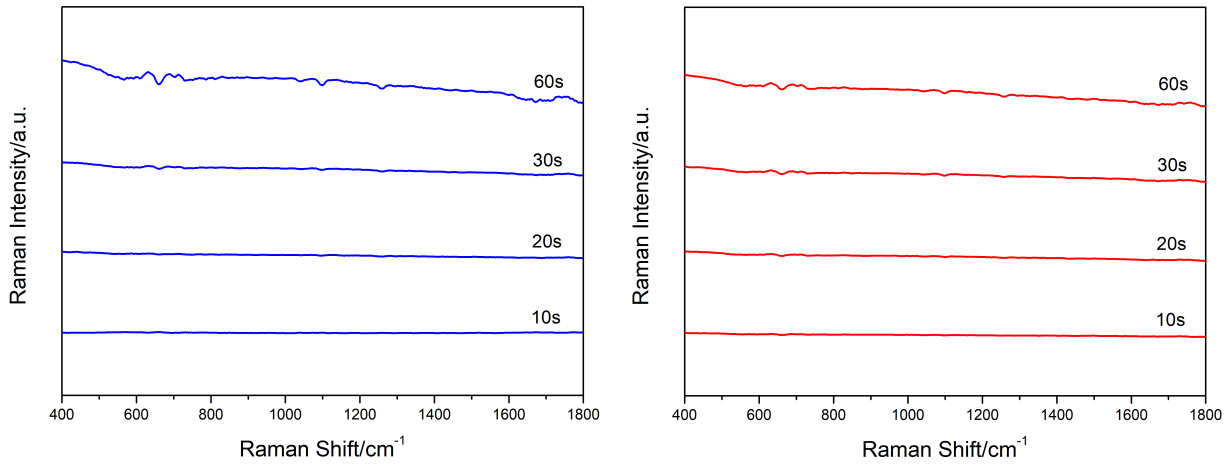

Fig. 2. The averaged conventional Raman spectra of serum samples: (a) healthy volunteers; (b) gastric cancer patients.

Figure 3 shows the comparison of the mean SERS spectra between 34 healthy volunteers and 34 gastric cancer patients, and the integration time for all samples is 10 s. It can be seen that the SERS spectra are considerably amplified relative to conventional Raman spectra. The inset in the upper portion of Fig. 3 shows the mean SERS spectra of serum of 34 healthy volunteers and 34 gastric cancer patients, the shaded areas represent the differences among individuals in the same group. The SERS spectra of both groups show good repeatability. The SERS spectra of both groups show intense peaks at 505 (attributable to isoleucine), 588 (attributable to ascorbic acid and amino compound), 644 (attributable to tyrosine), 722 (attributable to hypoxanthine), 861 (attributable to tryptophan), 1008 (attributable to phenylalanine), 1235 (attributable to D-mannose), 1397 (attributable to tryptophan), 1445 (attributable to elastin and collagen), 1586 (attributable to phenylalanine) and 1635 cm^{-1} (attributable to leucine). In order to better understand the biochemical information reflected in the serum SERS spectra at the molecular level, the main bands observed in the normal and gastric cancer SERS spectra and the corresponding assignment of biomolecules are listed in Table 1.[28–30]

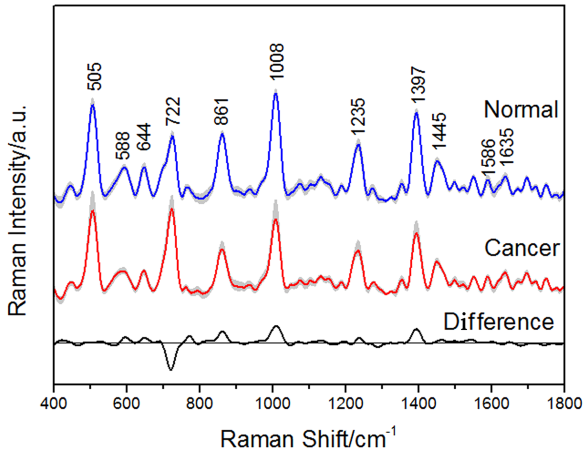

Fig. 3. Comparison of the mean SERS spectra for the normal serum ($n = 34$) vs that of the gastric cancer ($n = 34$). The shaded areas represent the standard deviations of SERS spectra of normal and cancer serum. The bottom spectrum corresponds to the difference of normal and cancer spectra.

The lower part of Fig. 3 shows the difference spectrum of the mean SERS spectra between healthy volunteers and gastric cancer patients, consider the biochemical differences among healthy volunteers, the Student's t-test was performed to ensure that the observed differences of peak intensity correspond effectively between normal and cancer patients. Nine SERS peaks with statistical significance ($p < 0.05$) were selected for analysis, that is 588, 644, 722, 861, 1008, 1235, 1397, 1445 and 1586 cm^{-1}. Comparing the intensities of these nine characteristic peaks reveals that the peak at 722 cm^{-1} in serum spectra of gastric cancer patients has high intensity. This peak is assigned to the in-plane bending vibration mode of the C–H bond of adenine in nucleic acid bases. This finding shows that the serum nucleic acid content of gastric cancer patients is higher than that of the healthy volunteers. The intensities of the characteristic peaks at 588, 644, 861, 1008, 1235, 1397, 1445 and 1586 cm^{-1}

Table 1. SERS peak positions and vibrational mode assignments and the comparison of the intensity of mean SERS spectra of normal and cancer (10^{-3}, mean ± s.d.).

Raman peak (cm^{-1})	Vibrational mode	Major assignment	Normal	Cancer	P
505	Ring vibration	L-arginine	17.31 ± 6.68	17.30 ± 7.02	0.0726
588		Ascorbic acid amide-VI	5.09 ± 0.81	3.93 ± 0.97	0.0264
644	ν (C–S)	Tyrosine	5.54 ± 0.57	4.60 ± 0.71	0.0301
722	ν (C–H)	hypoxanthine	11.93 ± 2.84	17.32 ± 3.14	0.0164
861	δ (C–O–H)	L-tryptophan	11.59 ± 0.46	8.98 ± 0.92	0.0203
1008	νs (C–C)	L-phenylalanine	16.86 ± 3.77	12.99 ± 3.95	0.0189
1235	ν (C–N)	D-mannos	10.42 ± 0.22	7.14 ± 0.43	0.0311
1397	δ (CH_2)	L-tryptophan	12.58 ± 1.66	10.57 ± 1.50	0.0195
1445	δ (CH_2)	Collagen, phospholipids	6.56 ± 0.09	5.55 ± 0.11	0.0445
1586	δ (C=C)	Phenylalanine	2.81 ± 0.09	2.77 ± 0.07	0.0451
1635	ν (C=O)	L-Leucine	5.42 ± 0.04	5.33 ± 0.06	0.0643

Notes: ν, stretching vibration; δ, bending vibration; νs, symmetric stretch.

in the serum spectra of gastric cancer patients are weaker than those of the same peaks in the serum spectra of healthy volunteers. The weak intensity of these peaks, which are attributable to carbohydrates and amino acids, indicates that the carbohydrate and amino acid contents of cancer patients are lower than those of healthy volunteers. The serum of patients with gastric cancer have elevated adenine contents and reduced protein contents because metabolism intensifies and large amounts of glucose and amino acids are consumed to provide the energy required by the excessive proliferation of cancer cells during carcinogenesis. The condition of abnormal metabolism is in line with the results of plasma detection using the SERS technique performed on nasopharynx cancer and gastric cancer by Feng *et al.*

Although the SERS spectra provided rich information, gastric cancer cannot be diagnosed accurately through the simple comparison of the characteristic peak intensities between healthy volunteers and gastric cancer patients. Therefore, it is necessary to further analyze the SERS spectral data by means of statistical methods to obtain better diagnosis results of gastric cancer.

3.2. *Analysis of SERS spectra of samples of gastric cancer patients and healthy volunteers*

3.2.1. *Principal component analysis*

Principle Component Analysis (PCA) is a multivariate statistical method commonly used to analyze the Raman spectra of different biological samples. Several principal components (PCs) with major contributions can be obtained by simplifying complicated spectroscopic data. These PCs characterize most spectral information and can be intuitively represented in two-dimensional and three-dimensional coordinates.

In this study, the polynomial fitting was used to subtract the fluorescent background of the original SERS spectral data. Then, PCA statistical analyses were performed on normalized spectroscopic data, and PC1, PC2, and PC4, the three PCs with the most significant differences, were selected through Student's t-test. The cumulative percentage variance of these three PCs is 83%.

As shown in Fig. 4, the two-dimensional scatter plot is drawn using PC1, PC2 and PC4 scores. Based on the combination of different significant principal component, most of serum samples of gastric cancer and healthy volunteers are clustered in two different areas. Figure 4(a) shows the PC1 and PC2 scatter plots for cancer and normal group data with the corresponding discriminant line, $PC2 = -2.11PC1+0.51$, and so 91.2% (31/34) sensitivity and 97.4% (33/34) specificity, with the accuracy of 94.1% (64/68); In addition, Fig. 4(b) shows the PC1 and PC4 scatter plot for cancer and normal group data with the corresponding discriminant lines, $PC4 = 2.83PC1\text{-}0.91$, and so 91.2% (31/34) sensitivity and 88.2% (30/34) specificity, with the accuracy of 89.7% (61/68). The result shows that the selection of different combinations of significant PCs will provide different levels of accuracy for serum classification.

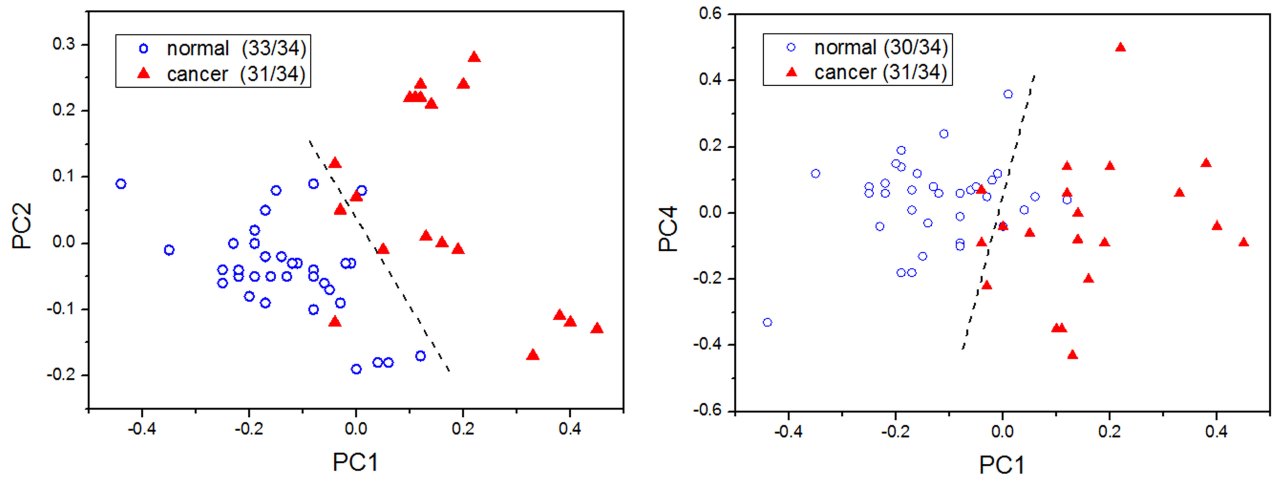

(a) (b)

Fig. 4. Scatter plots of the principal component (PC) scores for normal and gastric cancer serum spectra: (a) PC1 vs PC2; (b) PC1 vs PC4.

As shown in Fig. 5, the three-dimensional scatter plot is drawn based on PC1, PC2, PC4, and the sensitivity and specificity are 94.1% (32/34) and 94.1% (32/34) respectively, with the accuracy rate of 94.1% (64/68). From Fig. 5, it is clear that, although there is partial overlapping between normal and gastric cancer group, the two groups can be easily distinguished. The spatial distribution of the cancer group is relatively scattered while the normal group is relatively concentrated. This distribution pattern may be attributed to the stable serum component levels of the healthy volunteers given their normal physiological state. By contrast, the serum component levels of patients with cancer, who are in a pathological state, may drastically change. These results show that PCA can preliminarily discriminate the gastric cancer group from the normal group. Nevertheless, identifying the molecules that contribute to spectral differences is difficult, and the composition of human serum is complex. Therefore, PCA cannot be used to reflect negligible changes in the spectral shape and spectral intensity of serum SERS spectra.

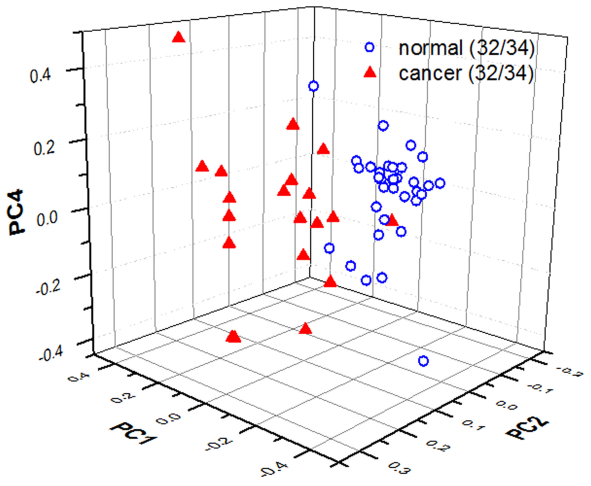

Fig. 5. (Color online) A three-dimensional scatter plot of the principal component (PC) scores of serum SERS spectra in gastric cancer (red triangle) and normal (blue circle) group.

3.2.2. *Characteristic ratio method*

SERS peaks attributable to different substances, such as proteins, fats, carbohydrates, and vitamins, reflect metabolic status and can be taken as important fingerprint peaks for cancer diagnosis.[31] Diseases have been diagnosed by analyzing the intensities of Raman characteristic peaks or the intensity ratios of different peaks. For example, the Raman intensity ratios of peaks at 1455 and 1655 cm^{-1} have been used to differentiate the serum of healthy volunteers from those of breast cancer patients and normal tissue from the tissue of malignant cervix neoplasm.[32,33] Lin *et al.* diagnosed colorectal adenocarcinomas by using the intensity ratio of SERS peaks at 725 and 638 cm^{-1}, which are attributable to adenine and tyrosine, respectively, as biological fingerprint information.

This study also attempted to use the peak intensity ratios of serum SERS spectra for the rapid diagnosis of gastric cancer. The four characteristic

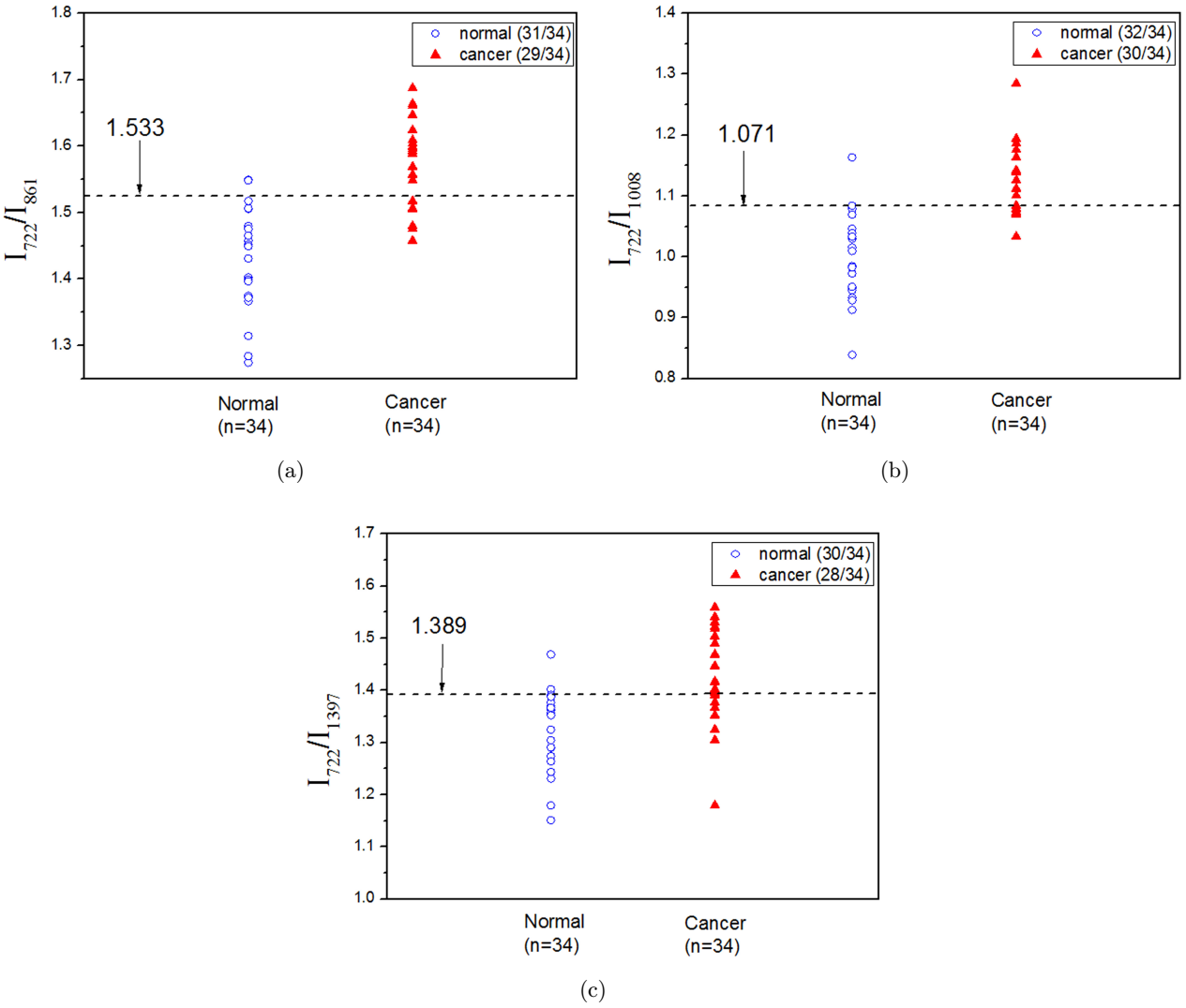

Fig. 6. Scatter plots of the intensity ratio of the Raman signal at (a) 722 vs 861 cm^{-1}; (b) 722 vs 1008 cm^{-1} and (c) 722 vs 1395 cm^{-1} as measured for each sample. The dotted lines ($I_{722}/I_{861} = 1.53$; $I_{722}/I_{1008} = 1.07$ and $I_{722}/I_{1397} = 1.39$) as diagnostic threshold detect the gastric cancer with 91.2% (31/34), 94.1% (32/34) and 88.2% (30/34) sensitivity, respectively; 85.3% (29/34), 88.2% (30/34) and 82.3% (28/34) specificity, respectively.

peaks at 722, 861, 1008 and 1397 cm^{-1} with the largest spectral difference (Fig. 3) and the most statistically significant difference identified through Student's *t*-test (Table 1) were selected for ratio analysis.

Figure 6(a) shows the one-dimensional plot using the I_{722}/I_{861} ratio and when the discriminant diagnostic line is 1.53, the discriminant sensitivity for the serum of cancer patients and healthy volunteers is 91.2% (31/34), and the specificity is 85.3% (29/34). Similarly, with $I_{722}/I_{1008} = 1.07$ and $I_{722}/I_{1397} = 1.39$ as diagnosis line, the sensitivities for the serum of cancer patients and healthy volunteers are 94.1% (32/34) and 88.2% (30/34), respectively, and the specificities are 88.2% (30/34) and 82.3% (28/34), respectively (see Figs. 6(b) and 6(c)). Therefore, using a single ratio index cannot sufficiently distinguish the serum of gastric cancer from that of healthy volunteers.

Figure 7(a) shows the two-dimensional plot, I_{722}/I_{1008} vs I_{722}/I_{861}, observing that the sensitivity and specificity are 100% (34/34) and 94.1% (32/34), with the accuracy of 97.1% (66/68). In addition, observing the two-dimensional plot, I_{722}/I_{1008} vs I_{722}/I_{1397}, in Fig. 7(b), the sensitivity and specificity are 94.1% (32/34) and 94.1% (32/34), with the accuracy of 94.1% (64/68). It is clear from Fig. 7 that there is slight overlaps between normal and

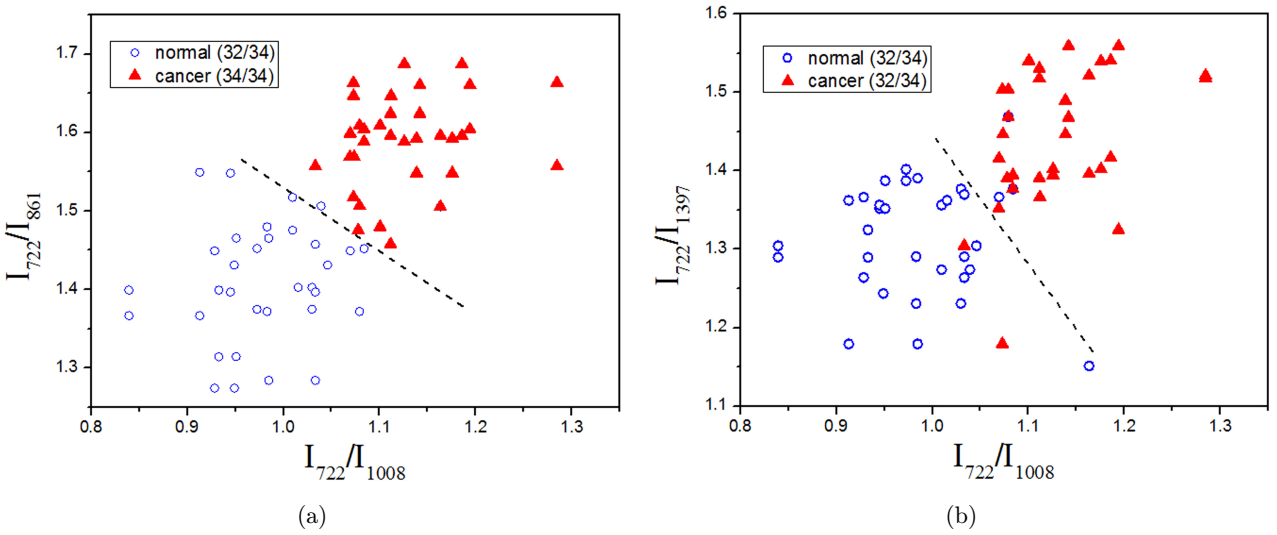

Fig. 7. Scatter plots of the intensity ratio of serum SERS spectra in gastric cancer and normal group: (a) I_{722}/I_{1008} vs I_{722}/I_{861}; (b) I_{722}/I_{1008} vs I_{722}/I_{1397}.

gastric cancer group, and the healthy volunteers can be easily differentiated from the gastric cancer patients. The spatial distribution of normal and cancer group is relatively concentrated.

The three-dimensional scatter plot based on the intensity ratios of I_{722}/I_{861}, I_{722}/I_{1008} and I_{722}/I_{1397} is shown in Fig. 8, and sensitivity and specificity are 100% (34/34) and 97.4% (33/34), respectively, with the accuracy of 98.5% (67/68). It is clear from Fig. 8 that the healthy volunteers can be easily differentiated from the patients with gastric cancer, and the space regions of cancer group and the normal group are distributed intensively. This result shows that the SERS spectral data of cancer patients can be directly differentiated from that of healthy volunteers on the basis of the peak intensity ratios with statistically significant differences, and that I_{722}/I_{861}, I_{722}/I_{1008} and I_{722}/I_{1397} can be used as the discriminant parameters for the identification of gastric cancer patients and healthy volunteers.

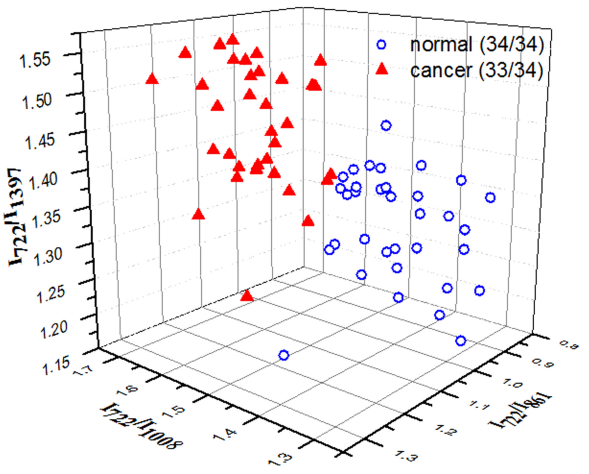

Fig. 8. A three-dimensional scatter plot of intensity ratio of serum SERS spectra in gastric cancer (red triangle) and normal (blue circle) group.

Comparing and analyzing Figs. 6–8 reveal that classification accuracy can be improved through the selection of multiple intensity ratios. Gastric cancer diagnosis based on SERS spectral data is a multifactor process that involves the extraction of multiple characteristics and not only a single ratio index. The above experiments were based on the intensity ratios of I_{722}/I_{861}, I_{722}/I_{1008} and I_{722}/I_{1397} from SERS spectra, and all these three ratios are significantly higher than that in normal serum. The intensity of SERS peaks at 861 cm^{-1} (attributable to tryptophan), 1008 cm^{-1} (attributable to phenylalanine) and 1397 cm^{-1} (attributable to leucine) weakened in the spectra of cancer serum. In contrast, the intensity of the peak at 722 cm^{-1} (attributable to adenine) is strengthened. It is indicated that the content and proportion of substances such as adenine in DNA and amino acids have changed in cancer serum, and proves that the canceration is a complex and multifactorial process, which is not only the result of abnormal metabolism of amino acids. This finding is the foundation of gastric cancer diagnosis based on SERS spectra combined with the CRM.

CRM is more suitable than PCA for the discrimination of serum SERS spectral of gastric

cancer. The peak intensity ratios of I_{722}/I_{861}, I_{722}/I_{1008} and I_{722}/I_{1397} reflect the abnormal metabolism of substances such as amino acids and nucleic acids in the serum of cancer patients, and can be considered as an important fingerprint peak for the early diagnosis and detection of gastric cancer. CRM shows the classified information of samples through the positions of each sample point in the band ratio classification map. Therefore, the classification results of CRM are more intuitive and operational than PCA, moreover, it shortens the time required for classification. With all these advantages, the physiological and pathological changes in the body metabolism can be reflected more efficiently and directly by CRM. The detection of biomolecular changes associated with cancer development is highly important for the early identification and diagnosis of gastric cancer.

4. Conclusions

In this paper, with gold nanoparticle as the enhancement base, the serum samples of gastric cancer patients are differentiated from that of healthy volunteers by SERS technique. The Raman intensity of the characteristic peak at $722\,cm^{-1}$ (attributable to adenine) in serum SERS spectra of gastric cancer patients is stronger than that in serum SERS spectra of healthy volunteers. In contrast, the Raman intensities of peaks at 588, 644, 861, 1008, 1235, 1397, 1445 and $1586\,cm^{-1}$, which are attributable to amino acids, phospholipids, and carbohydrates, in serum SERS spectra of gastric cancer patients are weaker than those in serum SERS spectra of healthy volunteers. Compared with serum samples of healthy volunteers, the protein structure in the cancer serum has changed, and the relative content of adenine increased while the relative content of phospholipid and carbohydrates decreased.

CRM and PCA are performed to analyze and discriminate the serum SERS spectra of healthy volunteers and gastric cancer patients. Results show that the classification performance of CRM is better than that of PCA, and the discrimination sensitivity and specificity are 100% (34/34) and 97.4% (33/34), respectively, with the accuracy of 98.5% (67/68). In contrast to PCA, which requires the use of integrated spectroscopic data, CRM can simply and directly use spectral information by selecting multiple peak intensity ratios. CRM may be applied as a rapid, simple, noninvasive blood detection method for gastric cancer with high accuracy and good popularization potential.

Conflict of Interest

The authors declare that there are no conflict of interest related to this article.

Acknowledgments

This work was supported by the Natural Science Foundation of Guangdong Province, China (2018 A0303131000), the project of Academician workstation of Guangdong Province, China (2014B0 90905001), the Fundamental Research Funds for the Central Universities, China (21617406) and the key project of Scientific and Technological projects of Guang Zhou, China (201604040007, 201604020168). We also gratefully acknowledge many of our colleagues for their stimulating discussions in this field.

Ethics

Serum samples were selected randomly collected from physical examination respondents of different departments of the First Affiliated Hospital of Jinan University. The research described in this paper was performed with full ethical approval and the patient was informed of the situation.

References

1. Y. Nie, K. Wu, J. Yu, Q. Liang, X. Cai, Y. Shang, J. Zhou, L. Pan, L. Sun, J. Fang, "A global burden of gastric cancer: The major impact of China," *Expert. Rev. Gastroent.* **11**(7), 651–661 (2017).
2. Z. Huang, S. K. Teh, W. Zheng, K. Lin, K. Y. Ho, M. Teh, K. G. Yeoh, "*In vivo* detection of epithelial neoplasia in the stomach using image-guided Raman endoscopy," *Biosens. Bioelectron.* **26**(2), 383–389 (2010).
3. S. K. Teh, W. Zheng, K. Y. Ho, M. Teh, K. G. Yeoh, "Near-infrared Raman spectroscopy for early diagnosis and typing of adenocarcinoma in the stomach," *Brit. J. Surg.* **97**(4), 550–557 (2010).
4. S. Duraipandian, M. S. Bergholt, W. Zheng, K. Y. Ho, M. Teh, K. G. Yeoh, J. B. Y. So, A. Shabbir, Z. Huang, "Real-time Raman spectroscopy for *in vivo*, online gastric cancer diagnosis during clinical endoscopic examination," *J. Biomed. Opt.* **17**(8), 081418 (2012).

5. J. T. Motz, S. J. Gandhi, O. R. Scepanovic, A. S. Haka, J. R. Kramer, R. R. Dasari, M. S. Feld, "Real-time Raman system for *in vivo* disease diagnosis," *J. Biomed. Opt.* **10**(3), 031113 (2005).
6. H. Zeng, J. Zhao, M. Short, D. I. Mclean, S. Lam, A. Mcwilliams, H. Lui, "Raman spectroscopy for *in vivo* tissue analysis and diagnosis, from instrument development to clinical applications," *J. Innov. Opt. Heal. Sci.* **1**(1), 95–106 (2008).
7. S. K. Teh, W. Zheng, D. P. Lau, Z. Huang, "Spectroscopic diagnosis of laryngeal carcinoma using near-infrared Raman spectroscopy and random recursive partitioning ensemble techniques," *Analyst* **134**, 1232–1239 (2009).
8. M. S. Bergholt, W. Zheng, K. Y. Ho, M. Teh, K. G. Yeoh, J. B. Y. So, A. Shabbir, Z. Huang, "Fiber-optic Raman spectroscopy probes gastric carcinogenesis *in vivo* at endoscopy," *J. Biophotonics.* **6**(1), 49–59 (2013).
9. A. Downes, A. Elfick, "Raman spectroscopy and related techniques in biomedicine," *Sensors.* **10**(3), 1871–1889 (2010).
10. M. Vendrell, K. K. Maiti, K. Dhaliwal, Y. T. Chang, "Surface-enhanced Raman scattering in cancer detection and imaging," *Trends. Biotechnol.* **31**(4), 249–257 (2013).
11. H. J. Butler, S. W. Fogarty, J. G. Kerns, P. L. Martin-Hirsch, "Gold nanoparticles as a substrate in bioanalytical near-infrared surface-enhanced Raman spectroscopy," *Analyst* **140**(9), 3090–3097 (2015).
12. Y. Wang, J. Irudayaraj, "Surface-enhanced Raman spectroscopy at single-molecule scale and its implications in biology," *Philos. T. R. Soc. B* **368**(1161), 20120026 (2013).
13. P. H. Hsua, H. K. Chianga, "Raman spectroscopy forquantitative measurement of lactic acid atphysiological concentration in human serum," *J. Raman. Spectroscopy.* **41**(12), 1610–1614 (2010).
14. S. K. Teh, W. Zheng, K. Y. Ho, M. Teh, K. G. Yeoh, Z. Huang, "Diagnosis of gastric cancer using near-infrared Raman spectroscopy and classification and regression tree techniques," *J. Biomed. Opt.* **13**(3), 034013 (2008).
15. R. Xiao, X. Zhang, Z. Rong, B. Xiu, X. Yang, C. Wang, W. Hao, Q. Zhang, Z. Liu, C. Duanb, K. Zhao, X. Guo, Y. Fan, Y. Zhao, H. Johnson, Y. Huang, X. Feng, X. Xu, H. Zhang, S. Wang, "Non-invasive detection of hepatocellular carcinoma serum metabolic profile through surface-enhanced Raman spectroscopy," *Nanomedicine* **12**(8), 2475–2484 (2016).
16. J. D. Guingab, B. Lauly, B. W. Smith, N. Omenetto, J. D. Winefordner, "Winefordner. Stability of silver colloids as substrate for surface enhanced Raman spectroscopy detection of dipicolinic acid," *Talanta* **74**(2), 271–274 (2007).
17. M. A. Cipriano, M. Areia, P. Amaro, M. Dinis-Ribeiro, M. A. Cipriano, C. Marinho, A. Costa-Pereira, C. Lopes, L. Moreira-Dias, J. M. Romaozinho, H. Gouveia, D. Freitas, M. C. Leitao, "External validation of a classification for methylene blue magnification chromoendoscopy in premalignant gastric lesions," *Gastrointest. Endosc.* **67**(7), 1011–1018 (2008).
18. S. Cervo, E. Mansutti, G. D. Mistro, R. Spizzo, A. Colombatti, A. Steffan, V. Sergo, A. Bonifacio, "SERS analysis of serum for detection of early and locally advanced breast cancer," *Anal. Bioanal. Chem.* **407**(24), 7503–7509 (2015).
19. H. Chon, S. Lee, S. W. Son, C. H. Oh, J. Choo, "Highly sensitive immunoassay of lung cancer marker carcinoembryonic antigen using surface-enhanced raman scattering of hollow gold nanospheres," *Anal. Chem.* **81**(8), 3029–3034 (2009).
20. S. Lee, H. Chon, J. Lee, J. Ko, B. H. Chung, D. W. Lim, J. Choo, "Rapid and sensitive phenotypic marker detectionon breast cancer cells using surface-enhanced Raman scattering (SERS) imaging," *Biosens. Bioelectron.* **51**, 238–243 (2014).
21. X. Li, T. Yang, S. Li, L. Jin, D. Wang, D. Guan, J. Ding, "Noninvasive liver diseases detection based on serum surface enhanced Raman spectroscopy and statistical analysis," *Opt. Exp.* **23**(14), 18361–18372 (2015).
22. D. Rohleder, W. Kiefer, W. Petrich, "Quantitative analysis of serum and serum ultrafiltrate by means of Raman spectroscopy," *Analyst* **129**(10), 906–911 (2004).
23. S. Fenga, R. Chen, J. Lin, J. Pan, Y. Wu, Y. Li, J. Chen, H. Zeng, "Gastric cancer detection based on blood plasma surface-enhanced Raman spectroscopy excited by polarized laser light," *Biosens. Bioelectron.* **26**(7), 3167–3174 (2011).
24. E. Vargas-Obieta, J. C. Martínez-Espinosa, B. E. Martínez-Zérega, L. F. Jave-Suárez, A. Aguilar-Lemarroy, J. L. González-Solís, "Breast cancer detection based on serum sample surface enhanced Raman spectroscopy," *Lasers Med. Sci.* **31**(7), 1317–1324 (2016).
25. S. A. Sánchez-Rojo, B. E. Martínez-Zérega, E. F. Velázquez-Pedroza, J. C. Martínez-Espinosa, L. A. Torres-González, A. Aguilar-Lemarroy, L. F. Jave-Suárez, P. Palomares-Anda, J. L. González-Solís, "Cervical cancer detection based on serum sample surface enhanced Raman," *Rev. Mex. Fis.* **62**(3), 213–218 (2016).
26. D. Lin, S. Y. Feng, J. J. Pan, Y. P. Chen, J. Q. Lin, G. N. Chen, S. S. Xie, H. S. Zeng, R. Chen,

"Colorectal cancer detection by gold nanoparticle based surface-enhanced Raman spectroscopy of blood serum and statistical analysis," *Opt. Exp.* **19** (14), 13565–13577 (2011).

27. H. Xiong, Z. Guo, H. Zhong, Y. Ji, "Monitoring the penetration and accumulation of gold nanoparticles in rat skin *ex vivo* using surface-enhanced Raman scattering spectroscopy," *J. Innov. Opt. Heal. Sci.* **9**(5), 1650026-1-11 (2016).
28. S. Feng, D. Lin, J. Lin, B. Li, Z. Huang, G. Chen, W. Zhang, L. Wang, J. Pan, R. Chen, H. Zeng, "Blood plasma surface-enhanced Raman spectroscopy for non-invasive optical detection of cervical cancer," *Analyst* **138**(14), 3967–3974 (2013).
29. P. Rekha, P. Aruna, G. Bharanidharan, D. Koteeswaran, M. Baludavidc, S. Ganesan, "Near infrared Raman spectroscopic characterization of blood plasma of normal, oral premalignant and malignant conditions-a pilot study," *J. Raman. Spectrosc.* **46**(9), 735–743 (2015).
30. S. X. Li, Y. J. Zhang, Q. Y. Zeng, L. F. Li, Z. Y. Guo, Z. M. Liu, H. L. Xiong, S. H. Liu, "Potential of cancer screening with serum surface-enhanced Raman spectroscopy and a support vector machine," *Laser. Phys. Lett.* **11**(6), 1–7 (2014).
31. S. K. Teh, W. Zheng, K. Y. Ho, M. Teh, K. G. Yeoh, Z. Huang, "Diagnostic potential of near-infrared Raman spectroscopy in the stomach: Differentiating dysplasia from normal tissue," *Brit. J. Cancer* **98**(2), 457–465 (2008).
32. J. L. Pichardo-Molina, C. Frausto-Reyes, O. Barbosa-García, R. Huerta-Franco, J. L. González-Trujillo, C. A. Ramírez-Alvarado, G. Gutiérrez-Juárez, C. Medina-Gutiérrez, "Raman spectroscopy and multivariate analysis of serum samples from breast cancer patients," *Laser Med. Sci.* **22**(4), 229–236 (2007).
33. U. Utzinger, D. L. Heintzelman, A. Mahadevan-Jansen, A. Malpica, M. Follen, R. Richards-Kortum, "Near-infrared raman spectroscopy for *in vivo* detection of cervical precancers," *Appl. Spectrosc.* **55**(8), 955–959 (2001).